

# A Novel Underactuated Robot Gripper With Scott-Russell Linkages for Human-Inspired Adaptive Grasp in Environmental Constraints\*

Shijie Qu, Che Zhang and Wenzeng Zhang

**Abstract**—This paper introduces Gamma-E gripper, a novel underactuated robotic gripper designed for adaptive desktop object manipulation, including thin-object scooping. The collision-resistant design enables automatic height adaptation through table-surface interaction, triggering passive finger flexion that transitions from parallel gripping to scooping mode upon reaching critical bending angles. The mechanism integrates Scott-Russell linkages with spring constraints, driven by a single linear actuator to achieve multi-modal operation: pinching, symmetric/asymmetric scooping, and adaptive enveloping. Its compact configuration allows integration with commercial robotic arms. Leveraging linear motion characteristics of the Scott-Russell linkage and geometric constraints, the gripper adaptively handles diverse objects while accommodating environmental constraints through inclined trajectories. This enables anthropomorphic adaptation to height variations, steps, and gradients. Symmetric scooping configuration excels at large thin objects, while asymmetric tilting enhances sheet-object stability. The design provides new perspectives for precision environment-adaptive grippers, expanding potential of underactuated systems in complex manipulation scenarios.

## I. INTRODUCTION

Grasping thin and flat objects in constrained environments remains a core challenge. Unlike many robotic grasping demonstrations that typically idealize grasping by placing objects in a suspended state, human fingers can not only naturally adapt to environmental constraints sliding across cluttered surfaces to grasp small objects but also automatically adjust their posture to ensure stable grasping when encountering environmental obstacles such as steps. Meanwhile, grasping strategies (e.g., pinching or enveloping) instinctively adapt to the optimal finger posture based on the size and shape of the object to achieve stable grasping. However, for most underactuated robotic hands composed of rigid bodies, human-like grasping under environmental constraints remains highly challenging, as their mechanical compliance is often limited by contact configurations and difficult to take effect.

Eppner [1] pointed out that leveraging the environment rather than avoiding it can yield robust and versatile grasping performance similar to that of human hands. They argued: "A competent gripper must exploit the constraints present in the environment through physical contacts to counteract uncertainties in the state variables most relevant to grasping

\*This research was supported by Natural Science Foundation of Top Talent of SZTU (Grant No. GDRC202334), the Program of E-SRT, ORIC, X-Institute.

Shijie Qu is with School of Artificial Intelligence, Shenzhen Technology University, Shenzhen, China and X-Institute, Shenzhen, China.

success." This concept provides an important insight for addressing the aforementioned challenges.

In recent years, numerous teams have been committed to solving the challenges of achieving stable grasping and scooping in unstructured scenarios. Some teams have focused on robotic arm control and algorithm design. For example, Jia [2] realized human-like robotic arm grasping in constrained environments using three complementary trajectory strategies. Kageyama [3] enabled traditional robotic arms to perform scooping actions after holding a spoon through algorithm design. These studies achieve scooping by developing robotic arm control algorithms.

On the other hand, other teams have explored whether the manipulator itself can achieve scooping. For instance, Dalle [4] designed serrated structures on the fingertips and used one finger to block the card, causing the object to flip over the fingertip. Zhang [5] conducted a study with a similar principle, realizing the scooping of sheet-like objects through the cooperative movement of two fingers. Lévesque [6] kept the angle of the robotic arm fixed and designed fingertips that can be inserted under objects for lifting.

Babin [7] introduced a passive joint based on this model, allowing the fingertips to actively bend to adapt to the desktop environment, thereby completing object grasping.

Cha [8] redesigned the mechanical fingertips based on an inclined robotic arm and accelerated the arm movement to achieve scooping by inserting the fingertips under the object. Mak [9] controlled the angle of the robotic arm and adopted a retractable finger mechanism to insert the fingertips under the object for scooping. He [10] used two spoon-like jaws combined with pneumatic actuation for food transfer.

Ko [11] installed a conveying device on the fingertips and realized in-hand manipulation using friction, which also enabled the grasping of objects such as tissue. In addition, many research teams have focused on the design of suction-based grippers. In the first Amazon Picking Challenge [12], many teams used suction-based grippers or added thin sheets with an angle of attack to the end of parallel jaws to simulate fingertip grasping. Some teams have also explored integrating electrostatic adsorption with suction in gripper design. However, suction cups and electrostatic adsorption still struggle to grasp objects with complex surfaces and usually require assistance from other fingers.

Che Zhang is with School of Artificial Intelligence, Shenzhen Technology University, Shenzhen, China (Corresponding author, email: zhangche@sztu.edu.cn)

Wenzeng Zhang is with Laboratory of Robotics, X-Institute, Shenzhen, China (Co-corresponding author, email: wenzeng75@163.com).

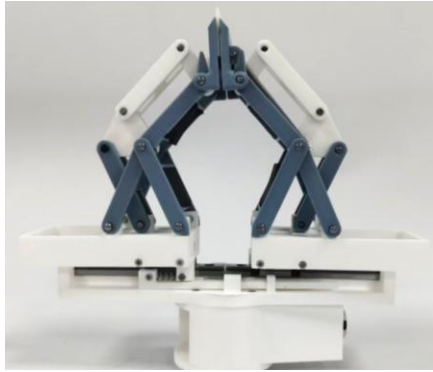


Figure 1. The Gamma-E gripper.

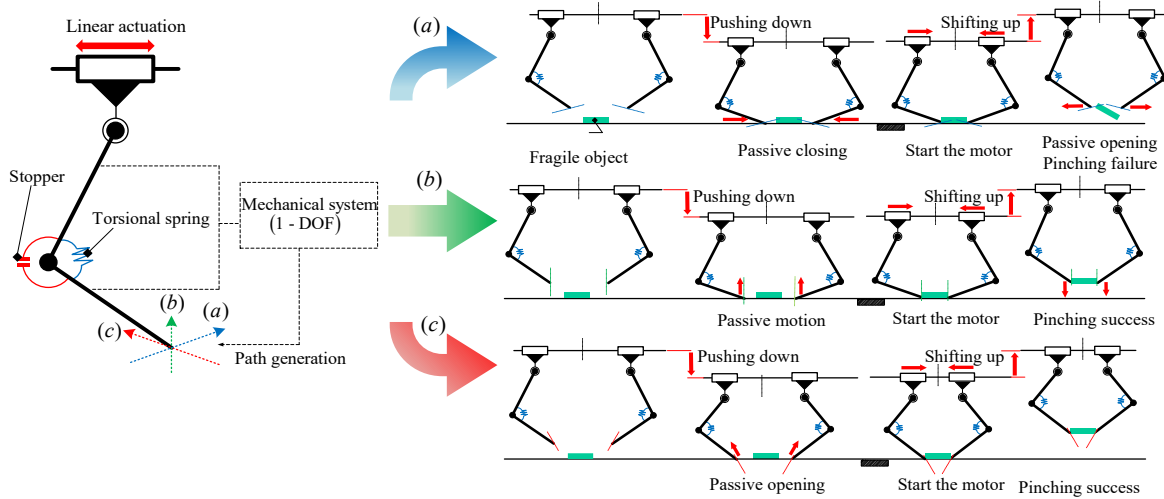


Figure 2. Possible movements of two - phalanx fingers based on fingertip paths. (a) Right diagonal path. (b) Vertical path. (c) Left diagonal path.

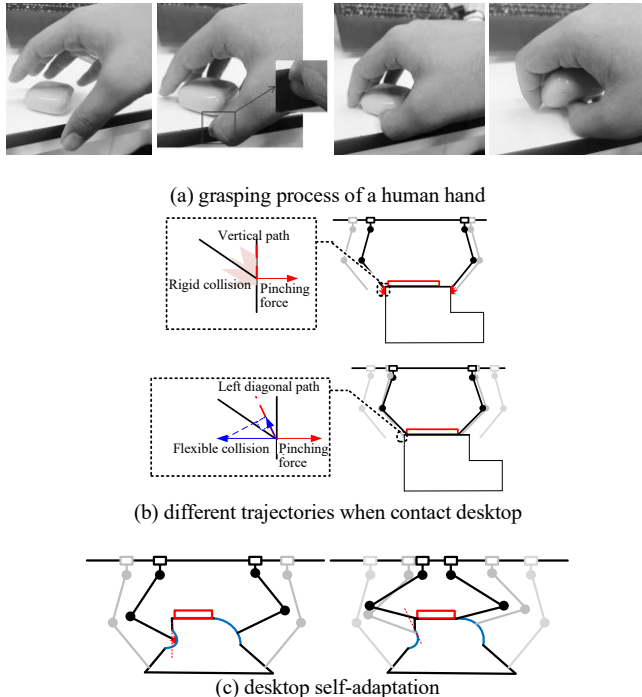


Figure 3. Fingers with a left-diagonal trajectory demonstrate superior adaptability to complex environmental constraints compared to those with a vertical trajectory, while more closely mimicking human-like grasping.

A study [13] integrated suction cups with viscous fluids, realizing the grasping of thin and light objects through suction force. It can be seen from the above studies that although many solutions for grasping thin and light objects have been developed, rigid collisions pose a major challenge to mechanical grippers, which usually rely on precise control.

To address the challenge of grasping thin and light objects, there is an urgent need to develop a mechanical gripper that is insensitive to rigid collisions, low-cost, simple to control, and capable of providing stable and powerful grasping. Following the idea of "leveraging the environment", Omega Hand of Yoon [14] has inspired research on flexible fingertip mechanisms for environmental interaction, providing new ideas for rigid manipulators to resist environmental impacts.

However, the OMEGA Hand has obvious shortcomings: its evaluation of the effectiveness of fingertip trajectories lacks empirical comparative analysis and appears arbitrary; the parameter design of the Hart linkage used to realize the linear trajectory of the end is overly complex with too many links, increasing manufacturing costs. Based on this research, we have explored and innovated the influence of different end trajectories on the adaptability to objects and the environment as well as the grasping effect, and have achieved the following key progress:

1. Based on the Scott-Russell linkage with preloaded springs, the fingertip motion trajectory exhibits a controllable inward-inclined characteristic. Its advantage lies in providing horizontal compliance when contacting the environment via the left diagonal path, avoiding rigid collisions. When lifting the object, the spring restoring force translates into a normal pressure component along the trajectory, enhancing grip of the fingertip on the object, enabling more stable grasping.

2. The Hart linkage is replaced by the Scott-Russell mechanism; the determination of its end trajectory does not rely on complex mathematical principles, and it can form a linear trajectory with an inclination angle of  $0\text{--}90^\circ$ .

We named this gripper Gamma-E (code: Gamma-E). Section II of this paper analyzes the principle of selecting an inwardly inclined trajectory for the distal phalanx. Section III

elaborates on the mathematical principles for determining the end trajectory of the Scott-Russell mechanism and introduces the mechanical structure and motion sequence of the gripper. Section IV provides a formulated model of the grasping force at the end of the Scott-Russell mechanism. Section V introduces the prototype and presents the results of grasping experiments. Finally, Section VI draws conclusions.

## II. INFLUENCE OF FINGERTIP TRAJECTORY ON GRASPING PERFORMANCE

Through design, the direction of the fingertip trajectory during environmental interaction can be predetermined. Figure 2 illustrates three classic fingertip grasping trajectories and their motion characteristics when interacting with planar surfaces.

If the fingertip moves along a right-diagonal trajectory, contact with the object will cause both fingertips of the parallel gripper to converge toward the interior of the grasping area, reducing the effective grasping range. Subsequently, when the robotic arm approaches from above and presses the gripper downward onto the supporting surface, the fingers bend under the support of the surface, causing spring deformation. At this point, the linear actuator can be activated to grasp the object. However, as the fingertips passively converge during the downward movement, improper placement of the gripper may lead to grasping failure due to the reduced range. Even after a successful grasp, if the linear actuator fails to maintain force on the fingertips, the spring will return the fingertips to their initial position, causing the object to fall.

If the fingertip follows a vertical trajectory, it can avoid the issues associated with the right-diagonal movement but can only adapt to flat, parallel surfaces. In environments with lateral protrusions or depressions, the vertical trajectory lacks lateral compliance and requires active torque to overcome obstacles. This may result in excessive contact forces or motion jamming. Achieving compliance in such cases still relies entirely on the control of the robotic arm, as shown in Figure 2(b).

Regarding the grasping method using the left-diagonal trajectory, literature [14] dismisses it with claims such as "the gripper cannot grasp objects with a width smaller than the initial opening distance of the fingertips."

However, simply adjusting the initial grasping position to the front of the finger base can avoid the so-called issue that "the gripper cannot grasp objects narrower than the initial opening distance of the fingertips." Furthermore, due to the action of the spring, the finger mechanism itself exerts a certain pressure on the object during grasping, enhancing gripping stability.

Inspired by the posture adjustment of the human hand when it touches the edge of a table while grasping an object (Figure 3a), we believe that good grasping under environmental constraints should not only adapt to changes in environmental height but also be adaptable to environments such as steps. Thanks to the left-diagonal trajectory, the movement direction of the fingertip includes both vertical and horizontal components. When encountering irregular surfaces:

1. The horizontal component can guide the fingertip to slide along the surface tangent or conform to the contour, reducing normal impact forces.

2. The vertical component maintains the necessary contact pressure.

The synergistic effect of these components enables the finger to follow surface undulations more smoothly, reducing the risk of jamming.

## III. OPERATING PRINCIPLE OF THE SCOTT-RUSSELL LINKAGE

To achieve the structure required for the left diagonal linear trajectory of the finger mechanism described above, we employed a straight-line mechanism — the Scott-Russell linkage. As shown in Figure 4, this mechanism is a link-slider assembly consisting of one slider and two links. Its uniqueness lies in satisfying the geometric relationship  $AB = BC = BD$ . Benefiting from this geometric constraint, its end trajectory is capable of generating linear motion along the AC direction. The operating principle of this mechanism is illustrated in Figure 4: Point B lies on the circumference of a circle centered at A with radius  $r$ ; the straight-line AC is always the chord of a circle centered at B with radius  $r$ . It is precisely based on this geometric relationship that precise linear motion is achieved.

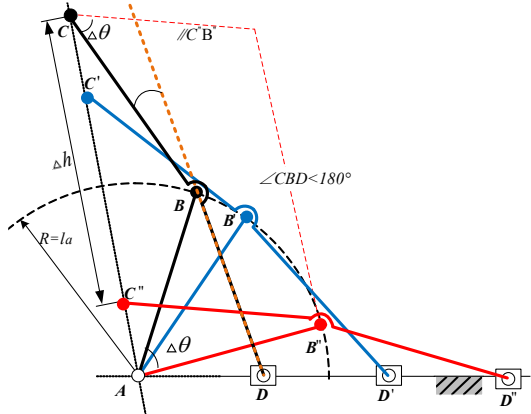


Figure 4. Principle of the Scott-Russell linkage.

### A. Linear Pinch Grip: Design of the Gamma-E gripper Based on the Scott-Russell linkage and Parallelolism Mechanism

Figure 4 shows the relationship between  $\Delta h$  and  $\Delta\theta$  when the Scott-Russell linkage is in vertical motion.

We define the linkage parameters as follows:  $l_{AB}$ ,  $l_{CB}$  and  $l_{AD}$  represent the length of the first finger segment, the second finger segment and the distance between the origin and the slide rail respectively.  $l_{CD}$  is the drive linkage, which enables the tip point C to move precisely along a straight line. The relationships among the parameters of these linkages can be obtained through formulas, so as to better set the initial state of the fingers and enable the fingers to better respond to external forces.

The mechanical characteristics of the Scott-Russell linkage itself are :

$$l_{CB} = l_{AB} = l_{BD} \quad (1)$$

In the initial state,  $l_{AD}$  satisfies the following relationship:

$$l_{AD} = 2l_{AB} \cos \angle BAD \quad (2)$$

The distance  $l_{AC}$  from the distal joint axis to the finger base satisfies:

$$l_{AC} = 2l_{AB} \sin \angle BAD \quad (3)$$

Set the length of the first finger segment as previously determined  $l_{AB} = 50\text{mm}$ ,  $\angle BAD = 70^\circ$ . The corresponding values of  $l_{AD} = 34.2\text{ mm}$  and  $l_{AC} = 93.97\text{ mm}$ , along with  $l_{AB}$ ,  $l_{AD}$ ,  $l_{AC}$ ,  $l_{CD}$  and angle  $\angle BAD$ , are stored in Table 1.

TABLE 1. Dimension Parameters of the Gamma-E finger.

Predetermined parameters		Designed parameters		
$l_{AB}$	$l_{CD}$	$\angle BAD$	$l_{AC}$	$l_{AD}$
50mm	10mm	$70^\circ$	93.97mm	34.2mm

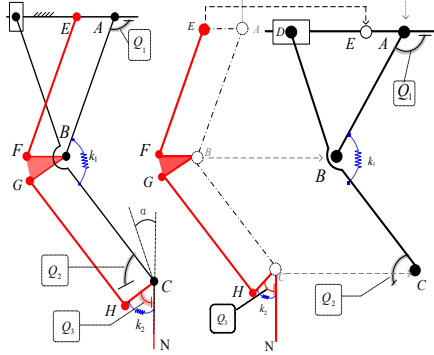


Figure 5. The Gamma-E finger with a Scott and a parallelogram mechanism.

In addition, as shown in Figure 5, a spring  $k_1$  is installed at joint B to enable the finger to extend after bending, achieving its compliance. A limit block  $Q_1$  is set at joint A, with  $Q_1=20^\circ$ , to ensure the stability of initial state of the finger.

#### B. Tip rotation: The implementation of the scooping method of the Gamma-E gripper.

As shown in Figure 5, the parallelogram mechanism and the Scott-Russell linkage share joints A, B and C. This arrangement makes the overall structure of the finger more compact. The stability of the parallelogram mechanism when gripping flat objects allows a pair of Gamma-E grippers to grasp objects more stably.

The fingertip of this manipulator can achieve two scooping postures in coordination with the robotic arm. Scooping can guide objects that cannot be directly grasped by flat clamping into the range where the gripper can grasp them and then perform pinching or enveloping operations.

A limit block  $Q_2$  is set on link CD and a limit block  $Q_3$  is set on link CH, with the angle designed as  $Q_3 = 52.5^\circ$  ( $\angle FBG = 40^\circ$ ). It works with spring  $k_2$  to provide vertical support for fingertip CN.  $Q_2$  is the key to triggering the scooping posture and its function and the conversion process of the scooping posture are shown in Figure 6. As shown in Figure 6, when the gripper is pushed downward and the height difference has not reached  $\Delta h_1$ ,  $Q_3$  and  $k_2$  can provide good support.

When the height displacement reaches  $\Delta h_1$ ,  $Q_2$  comes into contact with the fingertip. Further downward pressure can cause  $Q_2$  to push the fingertip to one side, forming an angle of attack, while overcoming the pressure of spring  $k_2$ . We can refer to  $0 \leq h \leq \Delta h_1$  as the flat clamping range.

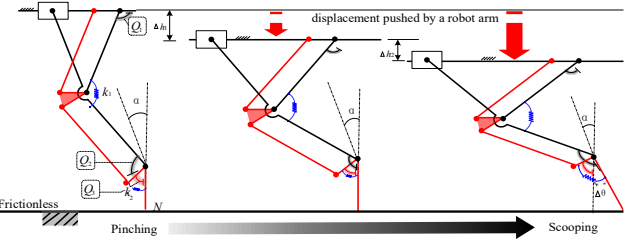


Figure 6. The fingertip posture transition from parallel pinching to scooping is achieved by the push of the limit block.

When the height displacement reaches and joint D reaches the end of the guide rail, the scooping posture is completed. We can refer to  $\Delta h_1 \leq h \leq \Delta h_2$  as the scooping range. The angle of  $Q_2$  is set to  $150^\circ$ . The size of the angle of attack is related to the angle setting of  $Q_2$  and the length l from the origin to the end of the track, satisfying:

$$\cos \theta = l / (2l_{oc}) \quad (4)$$

$$\theta = \arccos \theta \quad (5)$$

$$\Delta \theta = Q_2 - 90^\circ - \theta \quad (6)$$

Let the length l be 86.6 mm, at which point, when in the scooping posture,  $\theta$  is exactly  $30^\circ$ . In this case,  $\Delta \theta = 30^\circ$ . All dimensions of the parallelogram mechanism and the limit blocks are listed in Table 2.

TABLE 2. The Parallelogram Mechanism and the Limit Block.

$Q_1$	$Q_2$	$Q_3$	$\theta, \Delta \theta$	$\angle FBG$	$AE, BF, CH, BG$	$CN$
$20^\circ$	$150^\circ$	$52.5^\circ$	$30^\circ$	34.2mm	20mm	30mm

## IV. THEORETICAL ANALYSIS

The core functionality of this device lies in achieving stable scooping actions, with its key mechanism relying on the coordinated motion between the limit block  $Q_2$  and the distal fingertip during the scooping process. To ensure the reliability of the scooping motion, the following conditions must be satisfied: when the robotic arm is pressed downward into the target scooping range,  $Q_2$  must continuously push the fingertip to form a stable angle of attack, with no relative displacement between them. This constraint is essentially a static equilibrium problem, achieved through the rational configuration of the constrained force system acting on the fingertip, particularly the selection of the elastic coefficient  $k_2$  for the spring element. To better validate the grasping performance of the gripper and investigate the influence of different inclined trajectory angles  $\theta$  on the grasping force, we modeled the forces acting on the grasped object. The force model of the object satisfies the diagram in Fig. 9.

From the force diagram, we observe:

$$\begin{cases} f_R = \mu F_{R_x} \\ f_L = \mu F_{R_y} \end{cases} \quad (7)$$

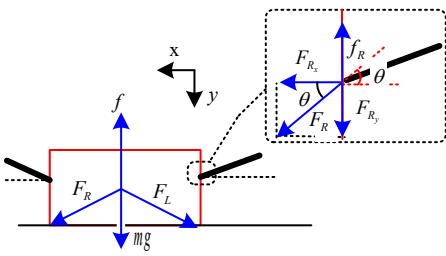


Figure 7. The relationship between grasping forces, frictions and angles.

Therefore:

$$f = f_L + f_R = mg + F_{R_y} + F_{L_y} \quad (8)$$

Based on the relationship of the forces, we obtain:

$$F_{R_y} / F_{R_x} = \tan \theta \quad (9)$$

Substituting Equation (9) into Equation (8), we readily derive:

$$\mu F_{L_x} + \mu F_{R_x} = mg + F_{R_y} + F_{L_y} \quad (10)$$

Thus:

$$\mu(F_{L_x} + F_{R_x}) = mg + \tan \theta(F_{R_x} + F_{L_x}) \quad (11)$$

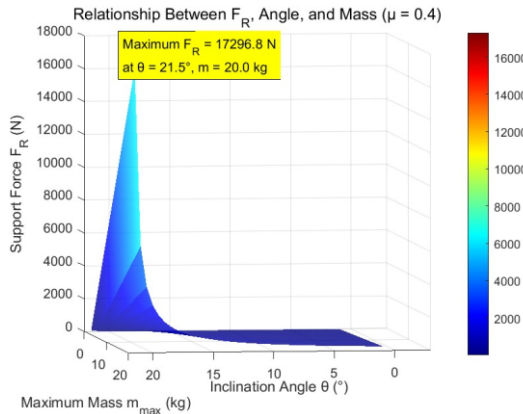


Figure 8. The relationship between  $F_R$ ,  $\theta$ ,  $m$ .

We arrive at the mechanical relationship relating the grasping force ( $F$ ), frictional coefficient ( $\mu$ ), and trajectory inclination angle ( $\theta$ ):

$$(F_{L_x} + F_{R_x})(\mu - \tan \theta) = mg \quad (12)$$

Let the maximum object mass that can be grasped be  $m_{\max}$ . Then we have:

$$2F_{R_{\max}} = m_{\max}g / (\mu - \tan \theta) \quad (13)$$

This yields the final relationship between  $F$ ,  $\mu$ , and  $\theta$ :

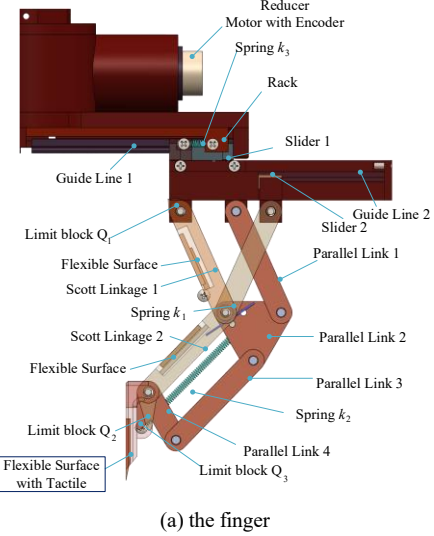
$$F_{R_{\max}} = m_{\max}g / (2(\mu - \tan \theta)\cos \theta) \quad (14)$$

Through formula analysis and visual plotting in MATLAB, we can see that a sudden change occurs when  $\theta$  is around  $20^\circ$ .

## V. GRASPING EXPERIMENTS

To validate the concept in the paper, a prototype was designed and utilized in grasping experiments to verify the environmental adaptability of the Gamma-E gripper and its

three grasping modes. Polylactic Acid (PLA) (Elastic Modulus: 3.5 GPa, Tensile Strength: 50 MPa) was prioritized in material selection due to its optimal balance between cost-effectiveness and functional requirements. A dimensional accuracy of 98.7% was ensured (achieved with a layer height of 0.1 mm and 25% hexagonal infill).



(a) the finger

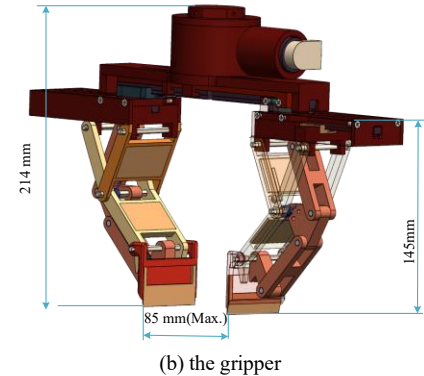


Figure 9. Overall view of the Gamma-E gripper.

### A. Prototype Design

As shown in Figure 9, the prototype of the Gamma-E gripper mechanism was designed based on the flange interface of a commercial robotic arm, enabling its mounting. A 2-mm-deep groove was designed on the contact surface between the Gamma-E fingertip and the object. A 2-mm-thick textured silicone pad was bonded within this groove to optimize surface interaction. Compared to bare PLA material, the textured silicone pad provides greater friction, enhancing grasping stability. Its elasticity also allows it to better simulate the mechanical characteristics of the human fingertip.

### B. Fingertip Adaptability to Environmental Constraints

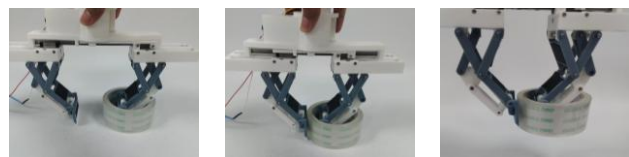
Grasping objects located at table edges or on stepped surfaces presents a significant challenge. The Gamma-E gripper, through its unique mechanical design driven by a motor, can overcome these height differences and grasp objects positioned at edges (as shown in Figure 10), mimicking the grasping process of a human hand in similar constrained environments.



Figure 10. The grasping process of Gamma-E Gripper.

### C. Pinch, symmetric and asymmetric scooping

The prototype successfully performed parallel grasping, symmetric scooping, and asymmetric scooping operations on smooth surfaces, as shown in Figure 11. In parallel grasping mode, it successfully grasped objects such as thin cards. In the case of symmetric scooping, it demonstrated adaptability to cylindrical objects, successfully repositioning a paper cup into a suitable orientation for enveloping grasp. Furthermore, the gripper can grasp irregularly shaped objects using its proximal and distal phalanges. For asymmetric scooping, by adjusting the tilt angle of the robotic arm, one fingertip is fixed on one side of the object, while the other side utilizes the angle of attack to slide beneath the object and lift it.



(a) Parallel grasping of objects



(b) Symmetric scooping of object



(c) Asymmetric scooping of a piece of card

Figure 11. Grasping experiments of the Gamma-E gripper.

the design utilizes the linear motion characteristics of the Scott-Russell linkage, replacing the traditional multi-link mechanism with a simplified four-link structure, which enables the mechanism to have compliance with an inward-inclined trajectory and realize grasping in stepped environments. Through the coupled design of a spring limitation mechanism and a parallelogram mechanism, the gripper can autonomously switch between four grasping modes: parallel grasping, symmetric scooping, asymmetric scooping, and adaptive enveloping, and has successfully completed stable grasping of cards and irregular objects in experiments.

### REFERENCES

- [1] C. Eppner, R. Deimel, J. Álvarez-Ruiz, M. Maertens, and O. Brock, “Exploitation of environmental constraints in human and robotic grasping,” *Int. J. Robot. Res.*, vol. 34, no. 7, pp. 1021–1038, 2015.
- [2] W. Jia, A. Ramirez-Serrano, Y. Liu. “Real-Time Interactive Capabilities of Dual-Arm Systems for Humanoid Robots in Unstructured Environments,” *IEEE Int. Conf. on Autom. Sci. and Eng.(CASE)*, Bari, Italy, pp. 474 – 481, Aug. 2024.
- [3] Y. Kageyama, M. Hamaya, K. Tanaka, et al., “Learning Scooping Deformable Plastic Objects Using Tactile Sensors,” *Int. Conf. on Autom. Sci. and Eng. (CASE)*, Bari, Italy, pp. 4020-4025, Aug. 2024.
- [4] L. U. Odhner, R. R. Ma, A. M. Dollar, “Open-Loop Precision Grasping with Underactuated Hands Inspired by a Human Manipulation Strategy,” *IEEE Trans. Autom. Sci. Eng.*, pp. 2830-2835, Jul. 2013.
- [5] Q. Zhang, Z. Hu, K. Koyama, et al. “Prying Grasp for Picking Thin Object Using Thick Fingertips,” *IEEE Robotics and Autom. Letters*, vol. 7, no. 4, pp. 11577–11584, Oct. 2022.
- [6] F. Lévesque, B. Sauvet, P. Cardou, et al., “A Model-Based Scooping Grasp for the Autonomous Picking of Unknown Objects with a Two-Fingered Gripper,” *Robotics and Autonomous Systems*, vol. 106, pp. 14–25, 2018.
- [7] V. Babin, D. St-Onge, C. Gosselin, et al., “Stable and Repeatable Grasping of Flat Objects on Hard Surfaces Using Passive and Epicyclic Mechanisms,” *Robotics and Computer Integrated Manuf.*, vol. 55, pp. 1–10, 2019.
- [8] H. Cha, I. Lee, J. Seo, “High-Speed Scooping Through Dynamic Manipulation: Model and Practice,” *IEEE Robotics and Autom. Letters*, vol. 10, no. 2, pp. 1377–1384, 2025.
- [9] K. H. Mak, J. Seo, “High-Speed Scooping Manipulation Using Controlled Compliance,” *RSS Workshop on High-Speed Robotics*, London, United Kingdom, pp.10261-10267, 2022.
- [10]T. He, S. Aslam, Z. Tong, et al., “Scooping Manipulation via Motion Control with a Two-Fingered Gripper and Its Application to Bin Picking,” *IEEE Robotics and Autom. Letters*, vol. 6, no. 4, pp. 6394–6401, Oct. 2021.
- [11]T. Ko, “A Tendon-Driven Robot Gripper with Passively Switchable Underactuated Surface and Its Physics Simulation-Based Parameter Optimization,” *IEEE Robotics and Automation Letters*, vol. 5, no. 4, pp. 5002 – 5009, 2020.
- [12]N. Correll, K. E. Bekris, D. Berenson, et al., “Analysis and Observations from the First Amazon Picking Challenge,” *IEEE Trans. Autom. Sci. Eng.*, vol. 15, no. 1, pp. 172–188, Jan. 2018.
- [13]A. Hajj-Ahmad, L. Kaul, C. Matl, et al., “GRASP: Grocery Robot’s Adhesion and Suction Picker,” *IEEE Robotics and Autom. Letters*, vol. 8, no. 10, pp. 6419–6426, Oct. 2023.
- [14]Yoon D., Kim K., “Fully Passive Robotic Finger for Human-Inspired Adaptive Grasping in Environmental Constraints,” *IEEE/ASME Trans. on Mechatronics*, vol. 27, no. 5, pp: 3841-3852. 2022.

### VI. CONCLUSIONS

This paper proposes an underactuated adaptive robotic gripper (Gamma-E gripper) based on the Scott-Russell linkage mechanism. Through mechanical innovation, this gripper achieves multi-modal grasping capabilities under environmental constraints. Experimental results show that: